ISSN (Print) : 0974-6846
Indian Journal of Science and Technology, *Vol 9(45), DOI: 10.17485/ijst/2016/v9i45/96938, December 2016* ISSN (Online) : 0974-5645

Numerical Analysis of the Hybrid Solar Collector Structure

R. Devaraj, S. Ramachandran*, G. Mageshwaran and K. Gobinath

Department of Mechanical Engineering, Sathyabama University, Chennai – 600119, Tamil Nadu, India;
r_devaraj67@yahoo.com, aishram2006@gmail.com, mageshwaran.mechanical@gmail.com, choicegobi@gmailcom

Abstract

Objective: The stability of supporting structure is designed for the hybrid solar collector that supports the parabolic collector and its accessories using finite element based simulation technique. **Methodology:** A supporting structure for supporting solar collector was designed and the simulation was carried out using ANSYS 15 tetrahedrons mesh control and the analysis is quite involved since loading is dynamic in nature due to the continuous movement of the tracking system. Throughout the design, the factor of safety is strictly restricted as 1 to avoid heavier structure and also to limit the structure cost. As a design improvement vertical and inclined cross members are attached to the ground support to withstand vibration. **Findings:** It is found that the vibration damping is good when the aperture is kept larger than the length of the collector. **Improvements:** The designed system can carry a load up to 800 kg. Therefore, the same structure can be used for an automatic tracking system.

Keywords: Collector Structure, Ground Support Structure, Hybrid Solar Collector, Simulation, Structural Analysis

1. Introduction

In[1] reported various reflective materials that can be used as reflective sheet by using variety of sources like FSEC solar library, web search engines, solar industry catalog's and directories, personal contacts, aluminum industry sources, solar cooker discussion groups and a wealth of other investigative resources. In[2] a high temperature change is measured when Reynolds' Wrap aluminum foil is used compared to the other materials like acrylic plate Plaskolite, Crystal Clear Polyethylene Film etc. This high reflectivity of this aluminum is highly suited for our experiment to produce more thermal and electrical output. In[3] demonstrated the use of plane mirror as reflective material in a parabolic trough. The reflectivity of mirror is very high but using curved mirror is not very costly, hence 110 plane mirrors of the following dimensions are used to obtain the parabolic trough. In[4] reported that a polymer mirror film consists of a silver reflective layer within multiple layers of polymer films protects the silver layer from oxidation and UV (Ultraviolet) degradation. In[5,6] reported that a pressure sensitive adhesive enables application to smooth, non-porous surfaces such as aluminum sheet. The film also has a peel-off protective mask that protects the mirror surface until the final reflector product is installed. Edge tape is used to protect film edges from long term exposure to wind, moisture and mechanical damage[7,8]. The comparative study of bare and ZnO/Si solar cells are carried out and also found that the coated cell has higher performance[9]. The heat transfer, temperature and efficiency have been studied by many researchers[10] from earlier days but the study of structural rigidity is started at later stage. Analysis of RC frame using ANSYS model shows the simulation power[11] and its simplicity in problem solving methodology. The application ANSYS simulation technique to electrical heating has been clearly shown in the study[12].

2. Methodology and Conceptual Design

As shown in Figure 1, the tracking system 1. Is connected to a wheel. 2. Which in turn is connected to the base, 3.

* *Author for correspondence*

Of the parabolic collector and 4. With the help of rack and pinion gear arrangement. The radius of the circular parabolic base is multiple times the radius of the wheel. A transparent tube (5) is placed above the parabolic reflector which acts as the receiver. The transparent tube (5) is covered by a dual layer of solar panels such that the inner solar panel (6) face the collector and the outer solar panel (7) face towards the sun. The entire setup is supported by a suitable support system. The construction of the system requires a tracking system. It is designed to rotate the collector at a rate of 30 degrees every half an hour. The movement of the tracking system (1) in turn makes the parabolic reflector (4) to move at a rate of 7.5 degrees every half an hour which is deduced to be the speed of the Sun and can hence track the Sun from the east to the west direction. The collector which is connected to the tracking system, tracks the Sun, collects the solar radiations and concentrates them at the focus of the parabola where the receiver i.e. the transparent tube (5) is placed. The focused beam heats the liquid flowing through the tube (5). The heated liquid such as water can be used for several industrial as well as household purposes. The infrared rays (cause of heat) from the concentrated solar rays are absorbed by the liquid flowing through the tube whereas the remaining photons (cause of light) are refracted by the water and spread uniformly on the inner solar panels 6. Since these refracted beams are consumed by the inner solar cells large amounts of voltage is obtained. The beams of sunlight blocked by the inner solar panels (6) is utilized by the outer solar panels (7), thus leading to the maximum consumption of the sun's rays thereby generating not only electricity but also heat, thus improving the overall efficiency.

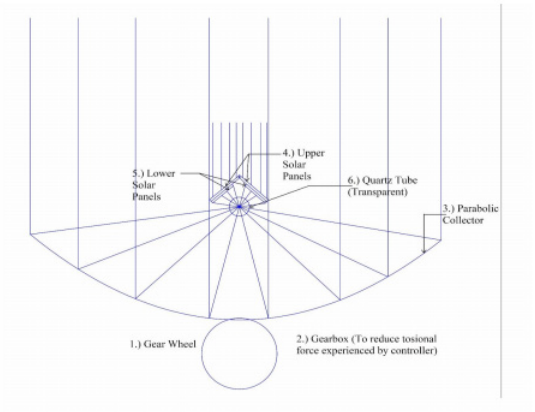

Figure 1. Schematic diagram of hybrid solar collector.

3. Initial Design of Hybrid Solar Collector

Figure 2 shows the preliminary design of the system. The above design is not satisfactory because there was a problem with the load applied on the centre tube support. The total load of the parabolic profile cannot be able to withstand on the structural design of the ground support. The structure when subjected to manual tracking might have greater impact on the ring of the ground support structure and the hinges located at the ends of the centre tube of support might break the ring, which may eventually collapse. The horizontal member perpendicular to the end of the base support is not provided. Therefore the whole system might undergo heavy vibration while moving the whole system on the wheel over the irregular surface, which might cause damages to its accessories such as quartz tube, solar panels (Table 1). Hence it has been decided to change the ground support structure and removing the hinges since the gear box location is coupled to one end of the centre tube support and the modeling is done similar to[13,14].

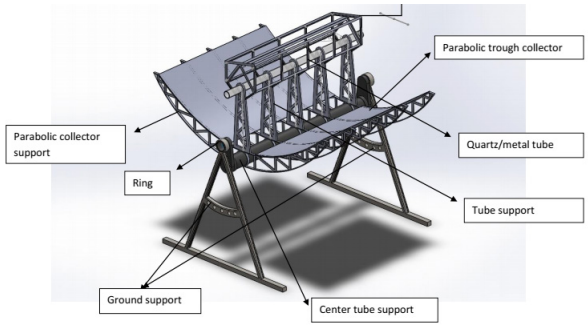

Figure 2. Design of hybrid solar collector.

4. Result and Discussion

4.1 Initial Ground Support Structure

The purpose of ground support is to carry the load of the parabolic profile and its accessories such as quartz tube support, quartz/metallic tube, solar panel and its structure. The height of the ground support is designed based upon the ultimate absorption of solar radiation falling on it. It is designed to receive and reflect maximum amount of solar radiation. Therefore there is a purpose for every dimension given to meet the required amount of output as per our estimation (Table 2).

Table 1. Mesh properties of ground support structure

Mass	Volume	Nodes	Elements	Moment of inertia At x-axis	Moment of inertia At y-axis	Moment of inertia At z-axis
23.29 kg	2.3293e-002 m^3	181880	115080	52.609 m^4	42.168 m^4	94.62 m^4

Table 2. Weight of the ground support is 228 kg

Moment of inertia	$I_x = \frac{bh^3}{12}$ $I_y = \frac{hb^3}{12}$
Weight of the each	F=mg
Volume of cylinder	$V = \pi r^2 h$
Component	V=b*h*L

The starting point for all modeling is "geometry". The geometry describes the shape of the model to be analyzed. The possibility of deformation occurrence in the whole structure of ground support when subjected to load is as shown in Figure 3. In Figure 4, the red fringes are formed on the ring of the center tube and on the adjacent member which means that at a particular load the possibility of deformation rate will be high at that particular region. A green fringe implies that deformation might initiate at that region. But might have negligible impact with load application and meshing is similar to[15].

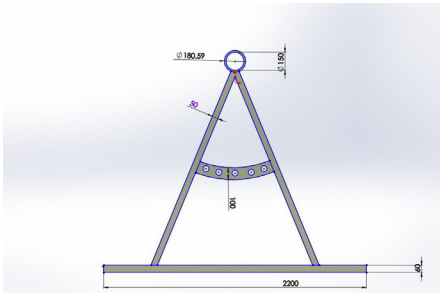

Figure 3. 2D Structure of ground support.

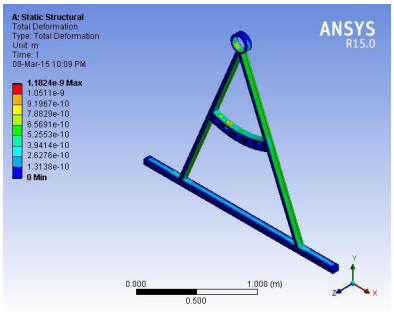

Figure 4. Total deformation.

The red fringes as shown in Figure 5 depict the direction of deformation. So even though the V-joints are welded rigidly, still the stress will be developing all around the ring, since the parabolic profile will undergo to and fro motion. The weight distribution must be varying on the innermost surface of the ring. So hence this structure may be a failure. The graph shown in the Figure 6 tells that the maximum deformation during loading and unloading takes place. It tell the changes in the structure when a pressure of 1569.06 Pa is applied on that particular surface. The maximum deformation is known to be 4.4919*10-10 m.

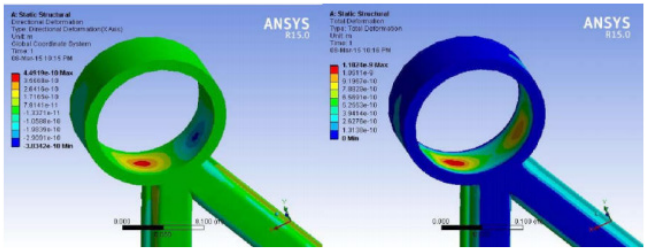

Figure 5. Directional deformation. and
Figure 6. Total deformation.

According to Figure 7, strain is distributed throughout the inverted "V" structure. As you can observe the edges and the adjacent curve member with yellow and red fringes which is due to the load distribution and in Figure 8 the strain energy is higher along the joints of the holes and also due to environmental stress this structure may not be considered as safe.

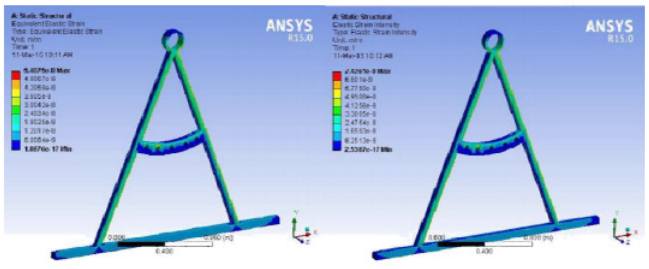

Figure 7. Shear elastic strain. and
Figure 8. Von-misses stress.

The stress intensity is observed on the edges of all the members of supports and the maximum pressure it

can withstand is 11425 pa as shown in Figure 9. Hence there is not much concern about it. But in Figure10, the maximum pressure it can withstand is 2148 Pa and our load is 1569 pa. Since it is coming close to that value, we can observe some red fringes developed on the edges.

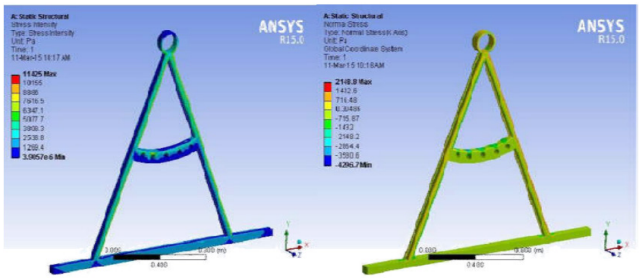

Figure 9. Stress intensity. and **Figure 10.** Normal stress.

As we can observe that strain developed on the support of the tube has exceeded the limit therefore strain might to cause deformation (Figure 11). It carries a load of 160 kg. and the thickness is just 50 mm. As per the study, it implies that deformations are likely to take place at the region with red fringes and the ground support might collapse due to over loading (Figure 12). The graph suggests that the load applied is constant over the period of time. Due to thermal stress, the rate of deformation may alter the longevity of the ground support structure. Hence the design is not safe and it not feasible (Table 3).

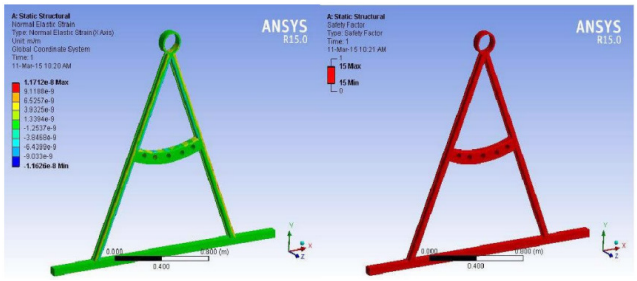

Figure 11. Normal elastic strain. and **Figure 12.** Safety factor.

Mesh properties of improved ground support
Surface area = 2920000.00 square millimeters

Weight = 470.4 kg

In the new improved design of the ground support, there are some cross members arranged in an inclined and vertical position to support the parabolic profile as shown in Figure 13, hence to overcome failure of the support, the welding of two different members are done in such a way to make it rigid and avoid vibration. It employs a different type of welding technique suitable for the material which is use to fabricate the whole system. Now to change the position of the whole system during the summer and winter lighting condition, a provision has been made to make the system mobile. So that it can move the whole apparatus to meet the ultimate lighting condition to give a clear understanding about the safe design of the ground support. The result obtained from the analysis using ANSYS gives us the required information in depth.

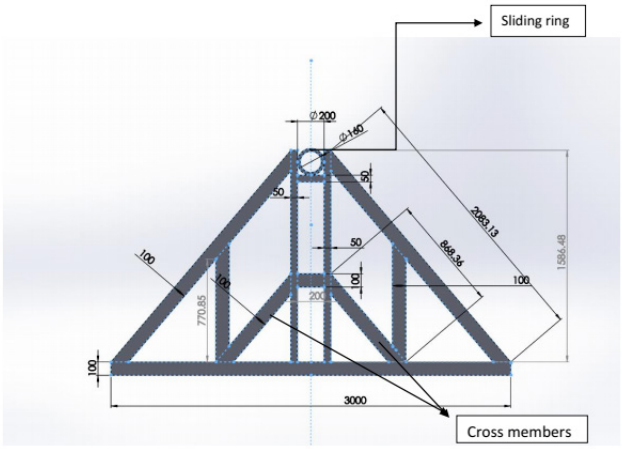

Figure 13. 2D structure of ground support with dimensions in mm.

4.2 Analysis using ANSYS 15.0

It is observed that, unlike the previous ground support, this design got some additional support due to presence of ground support, the only issue is on the ring, which develops some sort of deformation, hence it has been decided to increase the thickness which will most probably solve the issue (refer Figure 14).

Table 3. Improved design of the ground support

Mass	Volume	Nodes	Elements	Moment of inertia At x-axis	Moment of inertia At y-axis	Moment of inertia At z-axis
48 kg	4800000 c.c	390559	206321	104.01 m^4	246.27 m^4	350.09 m^4

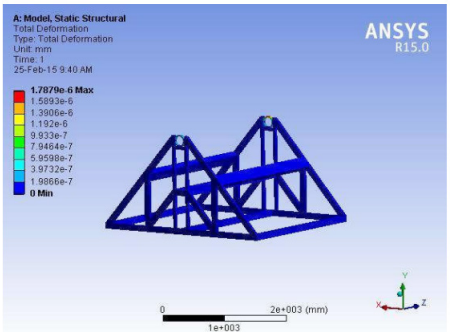

Figure 14. Total deformation.

As it is observed in Figure 15, the load distribution along all the members is found to be safe but the deformation in an around the ring is a bit disappointing therefore it is required to increase the thickness of the ring so that post deformation can be avoided.

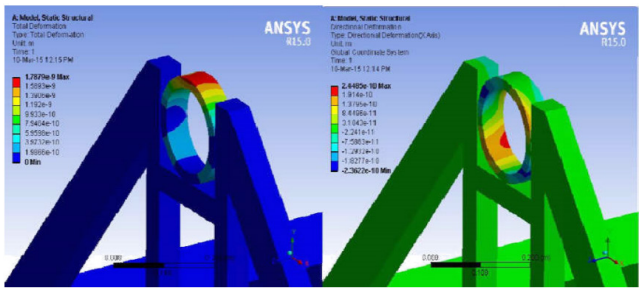

Figure 15. Total and directional deformation.

The rest of the report such as maximum shear stress in Figure 16, von-missis stress, elastic strain intensity, maximum shear stress are found to reach its safe level. In Figures 17 and 18, the stress is developed at the entire cross member but it is negligible which signifies safe design.

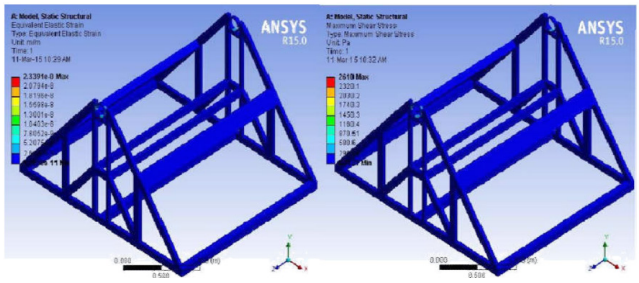

Figure 16. Von-missis strain and maximum shear stress.

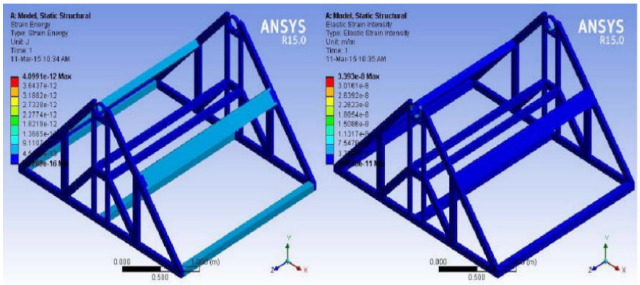

Figure 17. Strain energy distribution. and
Figure 18. Elastic strain intensity.

As shown in Figure 19 and Figure 20, when the load acting normally on the ground support structure, the strain is developed on the side horizontal members, hence the side members are removed. In Figure 21, the factor of safety which is found to be 1, it shows that it should not strictly exceed more than Figure 22and Table 4.

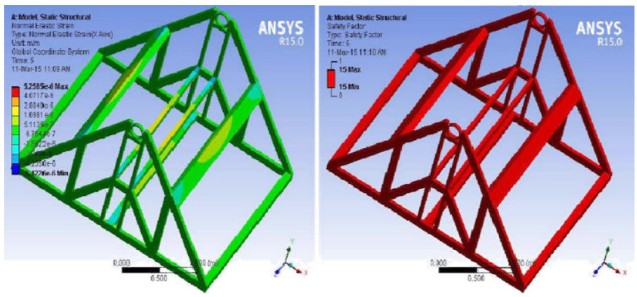

Figure 19. Normal elastic strain. and
Figure 20. Factor of safety.

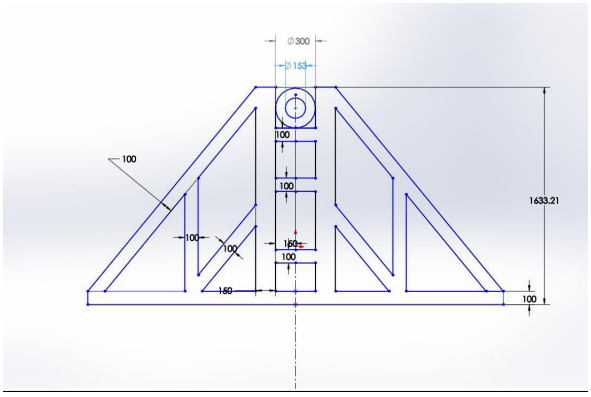

Figure 21. 2D sketch of ground support with dimensions in mm.

Table 4. Mesh properties of final ground support

Mass	Volume	Nodes	elements	Moment of inertia At x-axis	Moment of inertia At y-axis	Moment of inertia At z-axis
48 kg	4800000 c.c	391638	207645	104.01 m^4	246.27 m^4	350.09 m^4

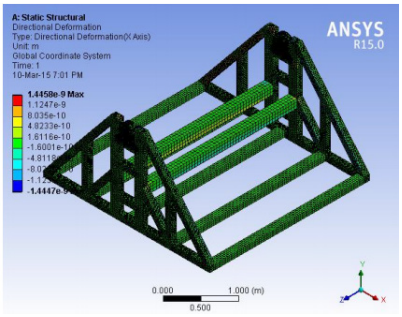

Figure 22. Total deformation.

4.3 Final Design of Ground Support

In Figure 23 and Figure 24, after the load application the elastic strain eventually developed on the side cross members, which is covered with green color, hence it is not much an issue.

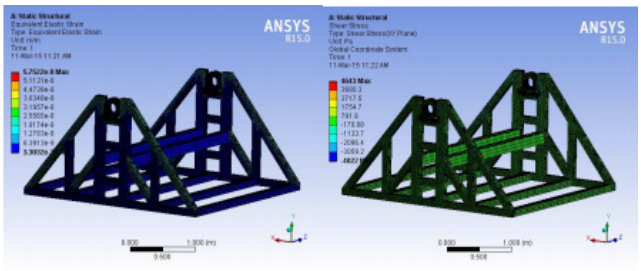

Figure 23. Equivalent elastic strain. and **Figure 24.** Maximum shear stress.

In Figures 25 and 26, the stress intensity is not much an issue, but the surface of the impact load generate some sort of stress which is quiet negligible, not evenly distributed throughout the surface. Hence the design is satisfactory.

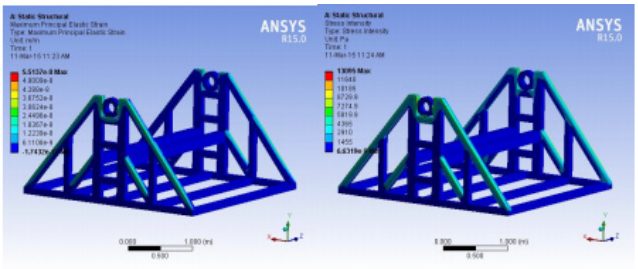

Figure 25. Maximum principle elastic strain. and **Figure 26.** Stress intensity.

In Figures 27 and Figures 28, the factor of safety is strictly restricted to 1 and cannot exceed more than that. Currently it has been made to track it manually. But the entire requirement for automatic tracking system in future over the same ground support has been provided. Hence there is hardly any changes needed. All the structures are made hollow and its thickness varies from 3 mm to 5 mm depending upon the load applied on it.

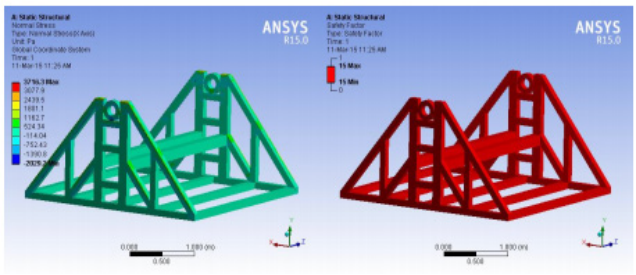

Figure 27. Normal stress. and **Figure 28.** Factor of safety.

5. Conclusion

This system is subjected to damping and vibration with larger aperture size than the length of the collector. So there will be more deflection. Hence it has to be made with extra supports. The factor of safety is strictly restricted to one and it should not exceed more than one. The tracking system is done manually. Also the parabolic reflector is rotated using worm wheel gear box. It is rotated to 7.5 degree for every 30 minutes. So the stress developed at the support is a complicated task since it is dynamic. Weight of the whole system is about 800 kg. The structural analysis of the whole structure is done and the result has been obtained and the design is found to be satisfactory.

6. References

1. Singh B, Singh M, Sulaiman F. Designing a solar thermal cylindrical parabolic trough concentrator by simulation. International Rio3 Congress. Rio de Janeiro: World Climate and Energy Event; 2003.
2. Reddy SV. Exergetic analysis and performance evaluation

of Parabolic Trough Concentrating Solar Thermal Power Plant (PTCSTPP). Energy Elsevier. 2012; 39:258–73.
3. Struckmann F. Analysis of a flat plate collector. Project Report MVK160. Lund, Sweden. Heat and Mass Transport. 2008; 8(3):451–86.
4. Folaranmi J. Design, construction and testing of a parabolic solar steam generator Leonardo Electronic Journal of Practices and Technologies. 2009; 7(14):115–33.
5. Jeter MS. Geometrical effects on the performance of trough collectors. Solar Energy. 1983; 30(2):109–13.
6. Hawlader M, Brinkworth B. An analysis of the non-convecting solar pond. Solar Energy. 1981; 27(3):195–204.
7. Mohammed BA. Design, fabrication and performance evaluation of an improved solar concentrating collectors using slat-mirrors. [MSc Thesis]. Zaria, Nigeria. Ahmadu Bello University. 2012; 2(1):822–30.
8. Stine WB, Harrigan RW. Solar energy fundamentals and design. New York. John Wiley and Sons Inc. 1985; 2(1):822–30.
9. Muhammed GS. Efficiency enhancement of crystalline silicon solar cell by the deposition of undoped ZnO thin film. Indian Journal of Science and Technology. 2011 Jun; 4(6):1–4.
10. Velmurugan P, Ramesh P. Evaluation of thermal performance of wire mesh solar air heater. Indian Journal of Science and Technology. 2011 Jan; 4(1):1–3.
11. Motwani P, Rajendhiran, Santhi AS. Simulation of brick infill and effect of openings on RC frames using ANSYS. Indian Journal of Science and Technology. 2015 Jan; 8(S2):1–7.
12. Farahani HF, Sabaghi M. Analysis of current harmonic on power system fuses using ANSYS. Indian Journal of Science and Technology. 2012 Mar; 5(3):1–5.
13. Mageshwaran G, Raja SKR, Sriram V. Biomechanics – reverse engineering of human bones for medical applications. International Journal of Applied Engineering Research. 2015; 10(11):10405–9.
14. Dudley VE, Kolb GJ, Mahoney AR, Mancini TR, Matthews CR, Sloan M, Kearney D. Test results: SEGS LS-2 solar collector. Report of Sandia National Laboratories (SAND-IA-94-1884); 1994. p. 1–22.
15. Raja SKR, Mageshwaran G. Analysis of hip femur joint for material polycaprolactone. Journal of Chemical and Pharmaceutical Sciences. 2015; 8(3):488–94. ISSN: 0974-2015.

Nomenclature

b	breadth (m)
h	height (m)
m	mass (kg)
g	acceleration due to gravity (m/s^2)
l	length (m)